Protection from hypertension in mice by the Mediterranean diet is mediated by nitro fatty acid inhibition of soluble epoxide hydrolase

Rebecca L. Charles[a], Olena Rudyk[a], Oleksandra Prysyazhna[a], Alisa Kamynina[a], Jun Yang[b,c], Christophe Morisseau[b,c], Bruce D. Hammock[b,c], Bruce A. Freeman[d], and Philip Eaton[a,1]

[a]King's College London, Cardiovascular Division, British Heart Foundation Centre of Excellence, The Rayne Institute, St. Thomas' Hospital, London SE1 7EH, United Kingdom; [b]Department of Entomology and Nematology, and [c]University of California, Davis Comprehensive Cancer Center, University of California, Davis, CA 95616; and [d]Department of Pharmacology and Chemical Biology, University of Pittsburgh School of Medicine, Pittsburgh, PA 15261

Soluble epoxide hydrolase (sEH) is inhibited by electrophilic lipids by their adduction to Cys521 proximal to its catalytic center. This inhibition prevents hydrolysis of the enzymes' epoxyeicosatrienoic acid (EET) substrates, so they accumulate inducing vasodilation to lower blood pressure (BP). We generated a Cys521Ser sEH redox-dead knockin (KI) mouse model that was resistant to this mode of inhibition. The electrophilic lipid 10-nitro-oleic acid (NO_2-OA) inhibited hydrolase activity and also lowered BP in an angiotensin II-induced hypertension model in wild-type (WT) but not KI mice. Furthermore, EET/dihydroxy-epoxyeicosatrienoic acid isomer ratios were elevated in plasma from WT but not KI mice following NO_2-OA treatment, consistent with the redox-dead mutant being resistant to inhibition by lipid electrophiles. sEH was inhibited in WT mice fed linoleic acid and nitrite, key constituents of the Mediterranean diet that elevates electrophilic nitro fatty acid levels, whereas KIs were unaffected. These observations reveal that lipid electrophiles such as NO_2-OA mediate antihypertensive signaling actions by inhibiting sEH and suggest a mechanism accounting for protection from hypertension afforded by the Mediterranean diet.

thiol | cardiovascular

Soluble epoxide hydrolase (sEH) has a conserved cysteine (Cys521) proximal to its catalytic center. This cysteine can undergo Michael addition with electrophilic lipids, which inhibits hydrolysis of the enzyme's epoxyeicosatrienoic acid (EET) substrates (1). This in turn elevates EET levels, which mediate blood vessel dilation and lowers blood pressure (BP), especially in the setting of hypertension (2, 3). Diverse sEH inhibitors limit injury in a variety of diseases (4), providing broad cardiovascular protection (5) against hypertension (6, 7), ischemia and reperfusion injury (8, 9), hypertrophy, and heart failure (10), as well as inflammation (11, 12). Consistent with the therapeutic potential of hydrolase inhibitors, sEH null mice are protected from pathological interventions (13). Conversely, genetic alterations that promote enhanced hydrolase activity are a risk factor for human heart failure (14).

The endogenous lipid electrophile 10-nitrooctadec-9-enoic acid (nitro-oleic acid, NO_2-OA) inhibits sEH in vitro (1). NO_2-OA and other fatty acid nitroalkenes appear to signal via pleiotropic mechanisms including targeting and activating peroxisome proliferator-activated receptor gamma (PPARγ), the Kelch-like erythroid cell-derived protein with CNC homology (EHC)-associated protein-1 (Keap1), and nuclear factor (erythroid-derived)-like-2 (Nrf2)-regulated antioxidant response genes and inhibiting proinflammatory gene expression regulated by nuclear factor kappa-light-chain-enhancer of activated B cells (NF-κB) (15, 16). Nitroalkenes are produced by radical addition of nitrogen dioxide (·NO_2) to one or more of the olefinic carbons of an unsaturated fatty acid. Nitrogen dioxide is both a product of oxidative inflammatory reactions involving nitric oxide (NO) and nitrite and the acidification nitrite. When the electron-withdrawing nitro group is bonded to alkenyl groups, this confers an electrophilic reactivity to fatty acids (17, 18). Thus, fatty acid nitroalkenes can modify proteins covalently via reversible Michael addition reactions that overall serves to link cellular metabolic and redox homeostasis with the posttranslational regulation of target protein function.

Nitro fatty acids, which have been detected endogenously in plasma and urine of humans, animal models, and plants (19–21), mediate salutary cardiovascular signaling actions (22). For example they relax blood vessels, attenuate platelet activation, and reduce inflammation via cyclic guanosine monophosphate (cGMP)-independent mechanisms (23, 24). Of relevance, the Mediterranean diet is characterized by high consumption of unsaturated fatty acids, especially from olive oil and fish rich in oleic and linoleic acid, together with vegetables rich in nitrite and nitrate (25). The acidic and low-oxygen conditions in the stomach provide an environment for efficient nitration of such unsaturated fatty acids by nitrite (26).

NO_2-OA normalizes blood pressure in an angiotensin (Ang) II-induced murine model of hypertension via undefined mechanisms (27). This was notable as pharmacological inhibitors of sEH also lower BP in murine hypertension, including salt- or Ang II-induced models (6, 7). As NO_2-OA inhibits sEH, we hypothesized that this mechanism may account for BP lowering in the setting of hypertension. Furthermore, as the Mediterranean diet both contains nitro fatty acids and can elevate their endogenous generation, this mechanism may contribute to

Significance

The Mediterranean diet is characterized by consumption of unsaturated fats with vegetables rich in nitrite and nitrate, resulting in endogenous formation of nitro fatty acids. These reactive lipids adduct to soluble epoxide hydrolase, inhibiting it to lower blood pressure. Mice genetically engineered to be resistant to this adductive inhibition had high blood pressure basally and their hydrolase activity was fully resistant to inhibition by nitro fatty acid supplied directly or generated via the Mediterranean diet. Similarly nitro fatty acid lowered blood pressure and abrogated cardiac hypertrophy in a hypertension model in wild-type mice, but was ineffective in mutant mice. Thus, protection from hypertension afforded by the Mediterranean diet is mediated by nitro-fatty acid-dependent inhibition of soluble epoxide hydrolase.

MEDICAL SCIENCES

dietary-induced BP decreases that in turn will reduce the risk of adverse cardiovascular event (28).

Given the complexity of causally establishing whether nitro fatty acids lower BP by inhibiting sEH, especially in the setting of dietary-induced endogenous fatty acid nitration, we generated a Cys521Ser sEH knockin (KI) mouse. This "redox-inactive" sEH thiol mutant, rendered insensitive to adductive inhibition by lipid electrophiles in vitro, provided a novel model system for testing the impact of lipid nitroalkenes on sEH hydrolysis of vasoactive EET species and downstream physiological responses (1). The data reveal that nitro fatty acids, applied exogenously as a pharmacological agent or generated endogenously as part of the Mediterranean diet, inhibit sEH to elevate plasma EETs, which in turn lower BP.

Results

NO_2-OA–Dependent Vasodilation Is Impaired in Cys521Ser KI Blood Vessels. NO_2-OA caused a dose-dependent vasodilation in isolated WT and KI mesenteric blood vessels. However, vasodilation to NO_2-OA was impaired in the KI, as indicated by a significant rightward shift in the response curve compared with the WT (Fig. 1A, $P < 0.05$). The half-maximal effective concentration (EC_{50}) for NO_2-OA was 113.9 ± 24.9 nM in WT compared with 354.5 ± 62.7 nM for KI vessels. This indicates the KI vessels are less sensitive to NO_2-OA than WT and is consistent with the anticipated phenotype, given the Cys521Ser sEH mutant was engineered to be resistant to adductive inhibition by lipid electrophiles. WT mesenteric vessels were incubated with or without the soluble guanylate cyclase inhibitor 1H-[1,2,4]oxadiazolo[4,3-a]quinoxalin-1-one (ODQ) and the dose-dependent relaxation responses to NO_2-OA were compared. ODQ did not alter the vasodilation induced by NO_2-OA alone (Fig. 1B).

NO_2-OA–Dependent Inhibition of sEH Is Deficient in Cys521Ser KI in Vivo. NO_2-OA or vehicle control was delivered systemically to WT or KI mice using osmotic minipumps. The hearts of mice were assessed for sEH activity, which was lower in KI than WT. This is consistent with previous observations that a Cys521Ser sEH mutant transfected into cells was less active than WT hydrolase (1). NO_2-OA significantly inhibited sEH activity in WT but not KI mice, consistent with the latter being deficient in the cysteine thiol target for lipid electrophile adduction (Fig. 1C).

NO_2-OA Abrogates Ang II-Induced Hypertension in WT but Not KI Mice in Vivo. The basal mean arterial pressure (MAP) was ~9 mmHg higher in KI mice compared with WT littermate controls (Fig. 2 A and B), consistent with a role for Cys521 of sEH in transducing vasodilatory responses of lipid electrophiles. Ang II increased MAP in both genotypes (Fig. 2 C and D), but this initial hypertensive response was potentiated by ~5 mmHg in KI compared with WT. Thus, Ang II increased MAP by 15 mmHg in WT compared with 20 mmHg in KI (Fig. 2 E and F). Administration of NO_2-OA reduced MAP in Ang II hypertensive WT mice, but was wholly ineffective in lowering BP in littermate KIs (Fig. 2 C–E and G).

Oxylipid Profile Analysis of Plasma Following Ang II and NO_2-OA Treatment. Plasma was collected from WT and KI mice basally and at the end of the Ang II + NO_2-OA treatment (as depicted in Fig. 2 C and D) for oxylipid profile analysis. EETs, dihydroxy-epoxyeicosatrienoic acids (DHETs) and hydroxy-eicosatetraenoic (HETEs) were measured by liquid chromatography tandem MS. Basally, there was no difference in 8,9-, 11,12-, or 14,15-ETT/DHET isomer ratios of WT compared with KI plasma. However, 15-HETE and 11-HETE were significantly decreased in KI compared with WT plasma. There was a similar tendency for plasma 8-HETE and 9-HETE to also be lower in KI than WT (Fig. 3A). Following the Ang II + NO_2-OA treatment, the 8,9-, 11,12-, and 14,15-EET/DHET isomer ratios were significantly higher in plasma from WT mice compared with KI mice ($P < 0.05$). The 5,6 EET/DHET ratio also showed the same
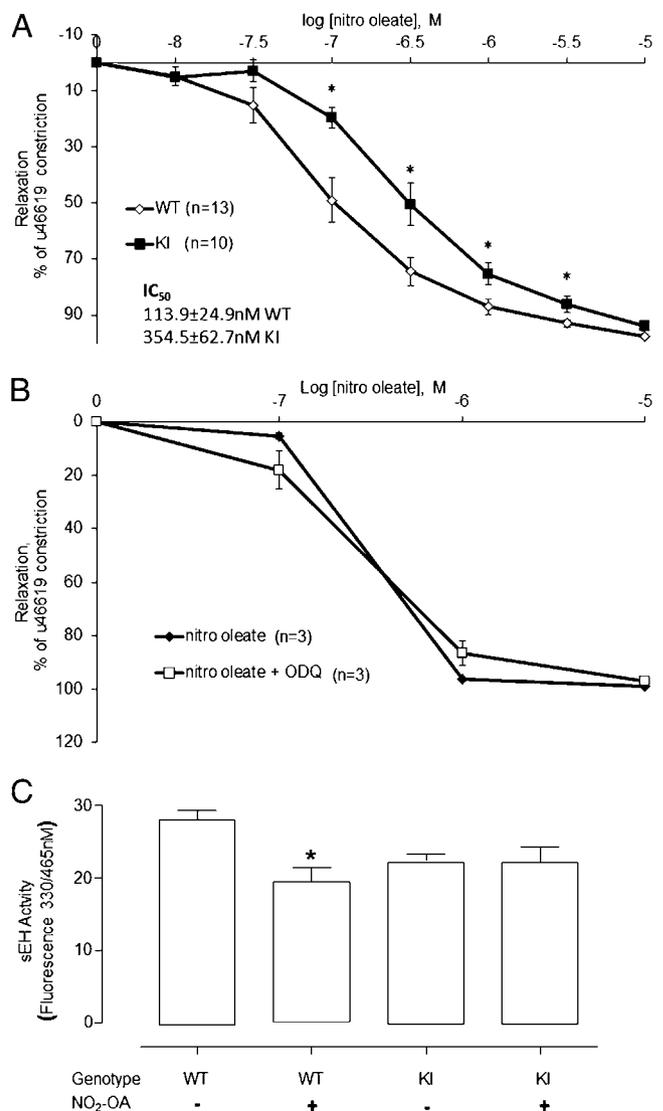

Fig. 1. Differential responses of WT and KI vessels to NO_2-OA. (A) WT or KI mesenteric vessels were constricted with the thromboxane mimetic U46619, and then increasing doses of NO_2-OA were added. The KI vessels showed a significantly impaired relaxation to NO_2-OA as indicated by their dose–response curve being shifted to the right compared with the WT. (B) NO_2-OA–dependent vasorelaxation was nitric oxide independent as the soluble guanylate cyclase inhibitor ODQ did not alter the dose–response curve. (C) sEH activity was assessed in hearts from WT or KI mice that had been implanted with an osmotic pump containing NO_2-OA or saline. NO_2-OA reduced sEH activity in WT but not in KI mice (*$P < 0.05$ ANOVA with post hoc t test).

tendency but differences did not reach statistical significance (Fig. 3B).

NO_2-OA Abrogates Ang II-Induced Hypertrophy in WT but Not Cys521Ser sEH KI. Consistent with Ang II inducing hypertension in WT as well as KI mice, the hearts from both genotypes became hypertrophic following this intervention (Fig. 3C). Ang II-induced hypertrophy in WT mice was abrogated by NO_2-OA, whereas this was ineffective in the KI (Fig. 3C). Again, the failure of NO_2-OA to combat Ang II-induced hypertrophy in KI mice was consistent with a failure to alleviate hypertension in this genotype (Fig. 2D).

NO_2-OA Adduction to WT but Not Cys532Ser KI sEH. A Western immunoblot-based assay that allows the stoichiometry of reversible
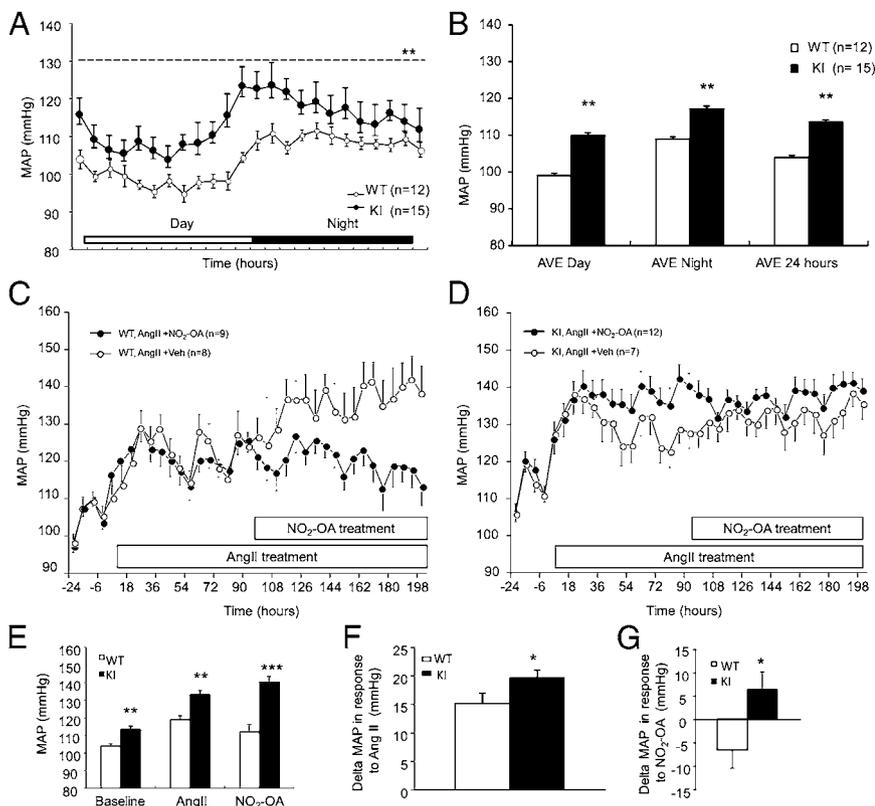
Fig. 2. KI mice are hypertensive compared with WT littermates. In vivo telemetric blood pressure monitoring compared KI mice with WT littermate controls. (A and B) MAP over time as 12-h time-averaged results showed KI mice were hypertensive compared with WT controls. (C–G) Ang II treatment increased BP in both genotypes, but this response was potentiated compared with KI. NO$_2$-OA abrogated Ang II-induced hypertension in WT mice, but had no impact in KI mice. Data are shown as mean delta MAP ± SEM following NO$_2$-OA treatment.

thiol modifications to be determined using an antibody to the protein of interest, in this case sEH, was undertaken. This procedure, known as the PEG-switch assay (29, 30), showed there was a basal level of reversible sEH modification in WT that was significantly increased following NO$_2$-OA treatment (Fig. 4A, $P < 0.05$). In contrast, KI mice showed no such increase (Fig. 4A), a consequence of the lack of the Cys521 thiol target.

Nitro Fatty Acids Are Formed from Dietary Components and Inhibit WT but Not KI sEH. The hearts of mice gavaged with conjugated linoleic acid (CLA) and sodium nitrite were assayed for sEH activity. This dietary intervention, which mimics aspects of the Mediterranean diet, significantly inhibited sEH activity in WT mice but not in KI mice (Fig. 4B, $P < 0.05$).

Further Characterization of the Cys521Ser KI Basal Phenotype. Additional studies characterizing the basal phenotype of the KI were undertaken. Hematological analysis of WT and KI showed there were no differences in blood biochemistry between WT and KI (Fig. S1A). Although KI mesenteric vessels were less sensitive to NO$_2$-OA than WT, there was no difference between genotypes in their vasodilatory responses to acetylcholine alone or acetylcholine in the presence of L-N^G-nitroarginine methyl ester (L-NAME) and indomethacin (Fig. S1B). Additionally, echocardiographic analysis showed there were no differences in basal heart function parameters between WT and KI (Fig. S1C).

Discussion

A number of sEH inhibitors lower BP by limiting the hydrolysis and inactivation of vasodilatory EETs (6, 7). The sEH is also inhibited by endogenously generated and exogenously administered lipid electrophiles. These thiol-reactive lipids covalently adduct Cys521 within the EET hydrolase domain to prevent hydrolysis to their corresponding DHETs (1). Electrophilic fatty acids are likely to display selectivity in sEH adduction because of structural homology with EET substrates, thus efficiently entering the hydrophobic catalytic domain of the hydrolase. Michael

addition reactions are modulated by the acid dissociation constant (pK$_a$) of the target thiol and steric interactions. However, in the case of sEH, spatial constraint of NO$_2$-OA within the enzyme's hydrophobic substrate domain (31) will likely augment the electrophile's interaction with the conserved Cys521 located in this domain, thus enhancing the efficiency of the adduction reaction.

Previous studies identified NO$_2$-OA as a lipid electrophile that readily inhibits sEH (1), as well as lowered BP in a model of Ang II-induced hypertension (27). As pharmacological inhibitors of sEH are known to be effective against hypertension (2, 3, 7), we reasoned that the BP-lowering effect of NO$_2$-OA was likely via adductive inhibition of sEH. NO$_2$-OA was selected for further study because of its endogenous presence, structural simplicity, and well-understood pharmacokinetics and metabolism (19, 20). Furthermore, NO$_2$-OA and other free and esterified fatty acid nitroalkenes are formed at elevated levels when unsaturated fatty acids are ingested together with a source of nitrite (26). Given the Mediterranean diet is high in both unsaturated fatty acids, for example from olive oil, as well as nitrite from vegetables, nitro fatty acid formation leading to sEH inhibition may contribute to BP-lowering and disease prevention provided by these dietary constituents. Given the complexities of addressing and establishing causal mechanisms related to nitro-fatty acid-mediated BP lowering, especially in the context of complex dietary-induced reactions, we generated a novel Cys521Ser sEH KI mouse line. This line, rendered "redox-null" due to the loss of a critical nucleophilic target, was anticipated to be resistant to inhibition by lipid electrophiles. This is a single atom alteration in sEH, in which the cysteine thiol (−SH) substituent is mutated to the hydroxyl (−OH) group of serine. Although this mutation is subtle, it prevents the adduction and inhibition of sEH by lipid electrophiles and manifests profound downstream physiological responses. By comparing the responses of WT and KI mice basally and in response to NO$_2$-OA, one is positioned to establish a causal relationship between sEH inhibition by lipid electrophiles and blood pressure lowering.
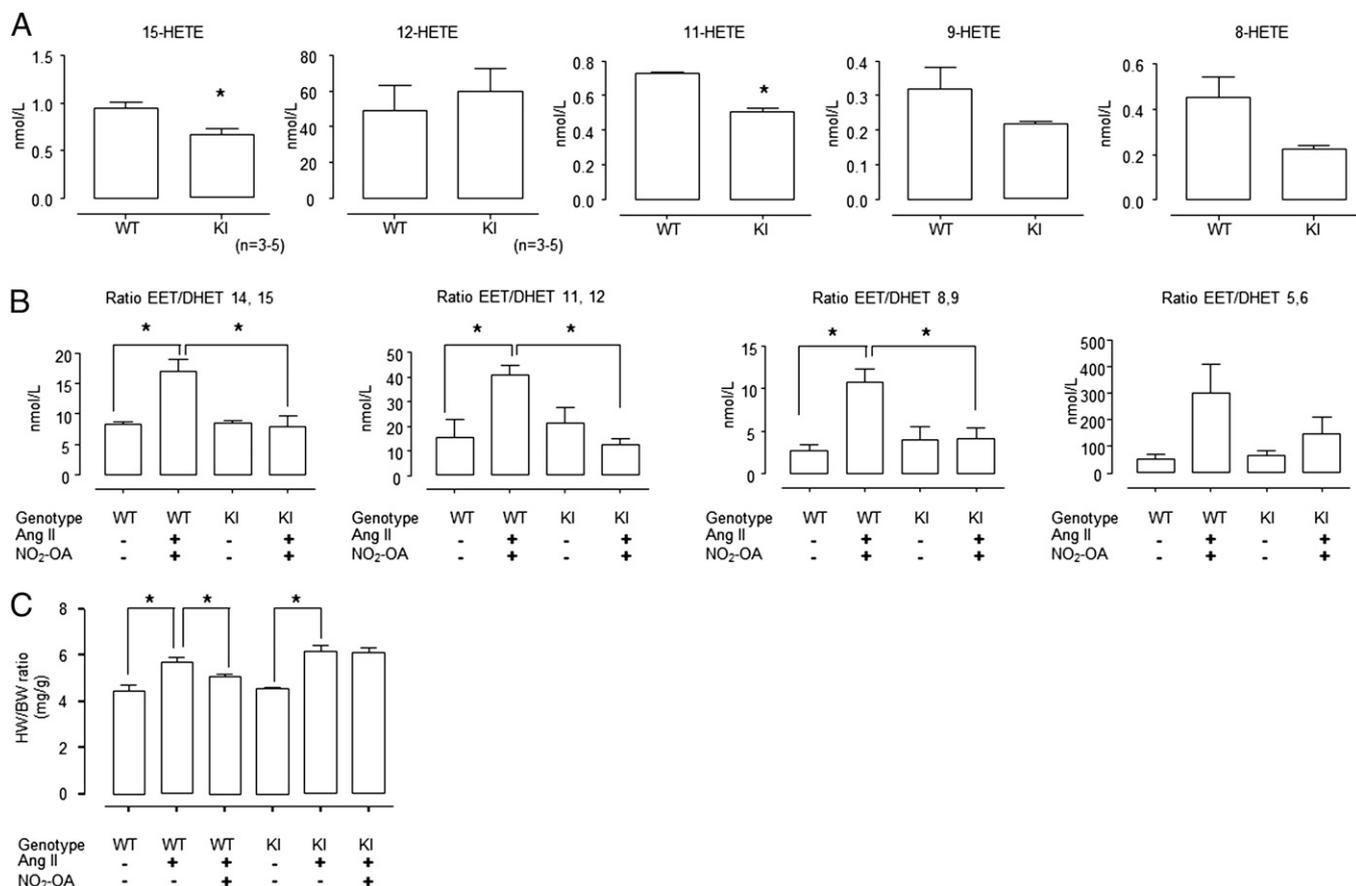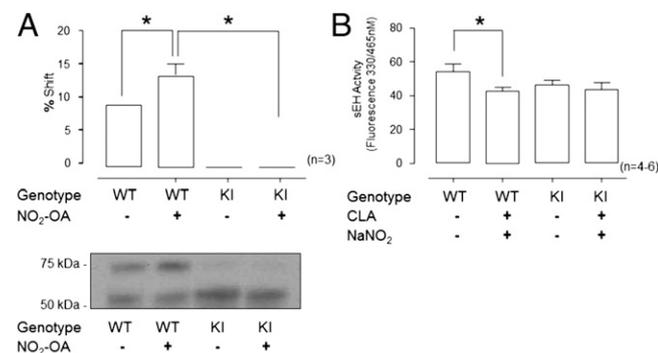
Fig. 3. EET/DHET ratio and HETE concentrations in plasma of WT and KI mice. (*A*) The 15-HETE and 11-HETE were significantly lower in the plasma of KI mice compared with WT, with 9-HETE and 8-HETE showing the same trend. (*B*) The plasma EET/DHET ratio increased in Ang II-induced hypertensive WT mice after NO$_2$-OA treatment but not in KI mice. (*C*) Hearts from WT mice treated with Ang II became hypertrophic, whereas KI mice displayed a slightly potentiated response. NO$_2$-OA attenuated Ang II-induced cardiac hypertrophy in WT mice and not in KI mice (*$P < 0.05$ ANOVA with post hoc *t* test).

Myography revealed the vasodilation of isolated mesenteric arteries in response to NO$_2$-OA, which was impaired in KI vessels compared with WT controls. These findings are rational as the KI was specifically engineered to lack Cys521 to be resistant to such electrophiles. It is controversial as to whether lipid nitroalkenes induce vessel relaxation in biological milieu via release of NO (32, 33). Herein, NO$_2$-OA–induced vasorelaxation was

Fig. 4. sEH displayed a reversible NO$_2$-OA–mediated posttranslational modification. (*A*) PEG-switch assay indicated this reversible modification of sEH, revealing that WT sEH has a low basal level of modification, which was enhanced in NO$_2$-OA–treated mice. In contrast, KI sEH was not modified and was resistant to modification by NO$_2$-OA. (*B*) Feeding mice CLA together with NaNO$_2$ significantly inhibited sEH activity in WT but not in KI mice.

unaffected by inhibition of soluble guanylate cyclase, the major target of NO. Thus, NO$_2$-OA does not relax vessels via cGMP-dependent mechanisms, an observation consistent with the inhibition of sEH by NO$_2$-OA and downstream elevation in EET levels. Although the EC$_{50}$ for NO$_2$-OA–dependent mesenteric relaxation for each genotype was determined in this study, the measured values require some further consideration because the modification by the electrophile is not readily reversible. Electrophile–protein adducts are likely slowly reversible or perhaps irreversible, which makes the adductive inhibition of sEH by NO$_2$-OA very time dependent. As a consequence, lower doses of the NO$_2$-OA provided over a longer time may induce the same amount of protein modification as a larger amount supplied for a short time. Indeed, with longer incubation times a low concentration of the electrophile 15-deoxy-delta-12,14-prostaglandin J$_2$, which also adducts Cys521 of sEH (1), has been shown experimentally to induce the same degree of labeling achieved acutely by a higher concentration (34). With these considerations in mind, the EC$_{50}$ for NO$_2$-OA–dependent mesenteric relaxation or sEH inhibition could substantively change, depending on the precise experimental conditions used, especially the time of exposure to the electrophile.

Next NO$_2$-OA or vehicle was delivered systemically to each genotype using an osmotic minipump. It was not feasible to measure sEH activity in mesenteries because of the limited amount of tissue that could be harvested. Consequently, sEH activity was measured in heart tissue, where NO$_2$-OA treatment was observed to inhibit hydrolase activity in WT but not KI. It was also noted that the sEH activity in the KI was slightly less than WT, consistent with previous studies in transfected cells

where it was observed that the cysteine-to-serine mutation similarly reduced EET hydrolysis (1). This suggests the explanation that the Cys521 thiol may provide protons necessary for EET hydrolysis and the addition of electrophiles to this thiol abrogates catalytic activity. Alternatively, the cysteine-to-serine mutation may induce a structural perturbation that reduces the efficiency of catalysis; an unlikely event given the mutation is subtle and conservative.

We found that the basal MAP of KI mice was ~9 mmHg higher than littermate WTs. This might be a consequence of endogenous electrophiles basally inhibiting the WT but not the KI. Indeed, when we used a PEG-switch assay to index reversible thiol modification of sEH, there was a basal level of cysteine modification that was further elevated following treatment with NO_2-OA. Moreover, both the basal and the NO_2-OA–induced modification was absent in the KI. However, there is additional complexity as we found that the activity of sEH in the KI was less than the WT, which is perhaps inconsistent with hypertension in the sEH redox-null mice. We note these hydrolase activity measurements and the PEG-switch assay, which was used to monitor the stoichiometry of modification by the electrophile, were performed with cardiac tissue, and not in resistance blood vessels, which was not technically possible. We quantified the basal EET levels in the plasma, but those measured were not different between genotypes and so they cannot account for the hypertension in the KI. However, there was a difference in the basal HETE levels in plasma from WT and KI mice. HETEs can cause vasorelaxation (35, 36), and therefore their decreased abundance in KI plasma provides an explanation for their basal hypertension compared with littermate WT. What remains undefined is the mechanism by which plasma HETE levels are lower in KI.

Ang II treatment increased BP in both genotypes, but the hypertensive response was potentiated in KI compared with WT mice. This is consistent with the presence of an endogenous lipid electrophile that inhibits WT sEH to offset the hypertensive response, but as this mechanism cannot operate in KI it has an exacerbated reaction to Ang II. Indeed, nitroalkenes and other electrophilic lipids may be produced endogenously in response to Ang II (37). When Ang II-induced hypertensive mice were administered NO_2-OA, BP was reduced in WT but not in KI mice. The striking failure of the NO_2-OA sEH to lower BP in hypertensive KI mice provides robust evidence that redox regulation of sEH by lipid electrophiles is an important regulator of BP in vivo, especially during hypertension. Perhaps the most compelling support for this concept comes from the measurement of plasma EET/DHET ratios in each genotype with or without NO_2-OA treatment. NO_2-OA increased the EET/DHET ratios in WT but not KI mice, consistent with the redox-null sEH variant being insensitive to modulation by lipid electrophiles. Overall, it is evident KI mice do not lower their BP in response to NO_2-OA because they cannot sense and transduce the net vasodilatory signaling actions of these electrophilic species.

Ang II treatment induced cardiac hypertrophy characteristic of the BP-elevating doses of this vasoconstrictive mediator. Consistent with NO_2-OA alleviating hypertension in WT mice via increasing EET levels, this intervention also limited hypertrophy. Furthermore, as NO_2-OA did not elevate EETs or lower BP in KI mice, it was ineffective in preventing cardiac hypertrophy. These observations are consistent with several studies that show pharmacological inhibition of sEH can limit cardiac hypertrophy secondary to hypertension (6, 14).

Although NO_2-OA clearly reduces BP in an Ang II-induced hypertension model, as well as the associated cardiac hypertrophy, it is notable that the extent of inhibition sEH activity caused by the electrophile was rather modest. It is difficult to define how much sEH inhibition is required to lower blood BP, but what is evident is that a number of vasodilatory EETs become elevated following this intervention in WT but not KI mice. Consequently, we can reasonably conclude that there was indeed sufficient inhibition of sEH to mediate the BP lowering. However, we are

also mindful that there could be additional, yet-undefined regulatory events that also contribute to the BP lowering and antihypertrophic effects of NO_2-OA. Another possibility to consider, although we have no evidence for such events, is that modification of Cys521 alters the product profile of the hydrolase.

Many credible mechanisms contribute to the epidemiological evidence of benefit from a Mediterranean-like diet (38, 39). The present findings support a new explanation for how cardiovascular protection can be afforded by a diet typified by consumption of unsaturated fats and vegetables abundant in nitrite and nitrate. Despite the Mediterranean diet being rich in fats that might promote cardiovascular disease, it protects against hypertension and associated risks (28). A key feature of the Mediterranean diet is the coconsumption of nitrite together with unsaturated fatty acid (e.g., from green leafy vegetables eaten with olive oil), promoting the further formation of sEH-inhibitory electrophilic fatty acid nitroalkenes that are also endogenously present in olives and olive oils (21). Indeed, when an unsaturated fatty acid was coadministered with sodium nitrite, using a protocol that elevates tissue nitro fatty acid levels (40), there was significant inhibition of sEH in WT but not KI mice. This mechanism for the endogenous generation of a sEH inhibitor providing cardiovascular protection is fully consistent with the actions of synthetic sEH inhibitors (41, 42). The findings of this study may provide an explanation, at least in part, for the findings of the Prevención con Dieta Mediterránea (PREDIMED) multicenter randomized trial (43), which showed a Mediterranean diet supplemented with extra virgin olive oil or nuts reduced the incidence of major cardiovascular events.

Finally, supplementation with nitrite or nitrate together and alone can also lower BP, a consequence of eventual reduction to vasodilatory NO and nitrosothiols (44, 45). It is also plausible that some of the effects of nitrite and nitrate may also be mediated by nitroalkene formation, as the host diet, intrinsic biosynthetic mechanisms, and commensal bacteria can produce an array of unsaturated fatty acids (46, 47).

Methods

More comprehensive methods are provided in *SI Methods*.

Generation of Cys521Ser sEH Knockin Mice. Mice constitutively expressing the sEH Cys521Ser mutation were generated on a pure C57BL/6 background by Taconic Artemis using a gene targeting vector.

Blood Biochemistry. Venous blood from WT or Cys521Ser KI mice was analyzed using a hand-held iSTAT analyzer, with EC8$^+$ cartridges (Abbott Laboratories).

Myography. Vascular rings were isolated from the mesenteric (second order) arteries and their responses to experimental interventions analyzed with a tension myograph (Danish Myo Technology).

Echocardiography. Age- and weight-matched littermate WT or Cys521Ser KI mice were anesthetized and examined by echocardiography using a high-resolution Vevo 770 echocardiography system (VisualSonics).

Telemetric Blood Pressure Monitoring in Vivo. BP was assessed by remote radiotelemetry in conscious freely moving mice as described previously (48–50).

Ang II-Induced Hypertension and NO_2-OA Delivery. Ang II with or without NO_2-OA was delivered by osmotic minipump (model 1007D) implanted s.c.

Soluble Epoxide Hydrolase Activity Assay. sEH activity was measured using the 3-phenyl-oxiranyl)-acetic acid cyano-(6-methoxy-naphthalen-2-yl)-methyl ester (PHOME; Cayman Chemical) assay.

Sample Preparation for Oxylipid Profiling Analysis. This analysis was carried out as previously described in detail (51), using liquid chromatography and tandem mass spectrometry.

Assay for Quantifying the Stoichiometry of NO_2-OA Adduction to sEH. This is based on a modified "PEG-switch" assay that allows the stoichiometry of

MEDICAL SCIENCES

reversible thiol oxidations to be determined using a Western blotting-based approach and an antibody to the protein of interest, namely sEH in these studies (29). The method, adapted to use β-mercaptoethanol (β-Me), has been used for the reductive labeling of proteins that adduct NO$_2$-OA (30).

Feeding Studies to Generate Endogenous Nitro Fatty Acids. Mice were gavaged daily for 5 d with conjugated linoleic acid and sodium nitrite in 200 μL PEG 400. This protocol has successfully increased endogenous nitro lipids in rodents (40), and models concentrations of key components of the Mediterranean diet. Control mice were gavaged with 200 μL PEG 400.

Statistics. Differences between groups were assessed using analysis of variance (ANOVA) where appropriate, followed by a *t* test. Differences were considered significant at the 95% confidence level.

1. Charles RL, et al. (2011) Redox regulation of soluble epoxide hydrolase by 15-deoxy-delta-prostaglandin J2 controls coronary hypoxic vasodilation. *Circ Res* 108(3):324–334.
2. Campbell WB, Harder DR (1999) Endothelium-derived hyperpolarizing factors and vascular cytochrome P450 metabolites of arachidonic acid in the regulation of tone. *Circ Res* 84(4):484–488.
3. Luria A, et al. (2007) Compensatory mechanism for homeostatic blood pressure regulation in Ephx2 gene-disrupted mice. *J Biol Chem* 282(5):2891–2898.
4. Marino JP, Jr. (2009) Soluble epoxide hydrolase, a target with multiple opportunities for cardiovascular drug discovery. *Curr Top Med Chem* 9(5):452–463.
5. Sasaguri T, Miwa Y (2004) Prostaglandin J2 family and the cardiovascular system. *Curr Vasc Pharmacol* 2(2):103–114.
6. Ai D, et al. (2009) Soluble epoxide hydrolase plays an essential role in angiotensin II-induced cardiac hypertrophy. *Proc Natl Acad Sci USA* 106(2):564–569.
7. Jung O, et al. (2005) Soluble epoxide hydrolase is a main effector of angiotensin II-induced hypertension. *Hypertension* 45(4):759–765.
8. Yeh CH, et al. (2006) Cardiomyocytic apoptosis following global cardiac ischemia and reperfusion can be attenuated by peroxisome proliferator-activated receptor alpha but not gamma activators. *Shock* 26(3):262–270.
9. Wayman NS, et al. (2002) Ligands of the peroxisome proliferator-activated receptors (PPAR-gamma and PPAR-alpha) reduce myocardial infarct size. *FASEB J* 16(9):1027–1040.
10. Imig JD (2006) Cardiovascular therapeutic aspects of soluble epoxide hydrolase inhibitors. *Cardiovasc Drug Rev* 24(2):169–188.
11. Schmelzer KR, et al. (2005) Soluble epoxide hydrolase is a therapeutic target for acute inflammation. *Proc Natl Acad Sci USA* 102(28):9772–9777.
12. Liu JY, et al. (2009) Inhibition of soluble epoxide hydrolase enhances the anti-inflammatory effects of aspirin and 5-lipoxygenase activation protein inhibitor in a murine model. *Biochem Pharmacol* 79(6):880–887.
13. Seubert JM, et al. (2006) Role of soluble epoxide hydrolase in postischemic recovery of heart contractile function. *Circ Res* 99(4):442–450.
14. Monti J, et al. (2008) Soluble epoxide hydrolase is a susceptibility factor for heart failure in a rat model of human disease. *Nat Genet* 40(5):529–537.
15. Schopfer FJ, et al. (2010) Covalent peroxisome proliferator-activated receptor gamma adduction by nitro-fatty acids: Selective ligand activity and anti-diabetic signaling actions. *J Biol Chem* 285(16):12321–12333.
16. Kansanen E, et al. (2011) Electrophilic nitro-fatty acids activate NRF2 by a KEAP1 cysteine 151-independent mechanism. *J Biol Chem* 286(16):14019–14027.
17. Ceaser EK, et al. (2004) Mechanisms of signal transduction mediated by oxidized lipids: The role of the electrophile-responsive proteome. *Biochem Soc Trans* 32(Pt 1):151–155.
18. Freeman BA, et al. (2008) Nitro-fatty acid formation and signaling. *J Biol Chem* 283(23):15515–15519.
19. Baker PR, Schopfer FJ, Sweeney S, Freeman BA (2004) Red cell membrane and plasma linoleic acid nitration products: Synthesis, clinical identification, and quantitation. *Proc Natl Acad Sci USA* 101(32):11577–11582.
20. Lima ES, Di Mascio P, Rubbo H, Abdalla DS (2002) Characterization of linoleic acid nitration in human blood plasma by mass spectrometry. *Biochemistry* 41(34):10717–10722.
21. Fazzari M, et al. (2014) Olives and olive oil are sources of electrophilic fatty acid nitroalkenes. *PLoS One* 9(1):e84884.
22. Rudolph V, et al. (2010) Endogenous generation and protective effects of nitro-fatty acids in a murine model of focal cardiac ischaemia and reperfusion. *Cardiovasc Res* 85(1):155–166.
23. Coles B, et al. (2002) Nitrolinoleate inhibits superoxide generation, degranulation, and integrin expression by human neutrophils: novel antiinflammatory properties of nitric oxide-derived reactive species in vascular cells. *Circ Res* 91(5):375–381.
24. Coles B, et al. (2002) Nitrolinoleate inhibits platelet activation by attenuating calcium mobilization and inducing phosphorylation of vasodilator-stimulated phosphoprotein through elevation of cAMP. *J Biol Chem* 277(8):5832–5840.
25. Weitzberg E, Lundberg JO (2013) Novel aspects of dietary nitrate and human health. *Annu Rev Nutr* 33:129–159.
26. Napolitano A, et al. (2004) Acid-induced structural modifications of unsaturated fatty acids and phenolic olive oil constituents by nitrite ions: A chemical assessment. *Chem Res Toxicol* 17(10):1329–1337.
27. Zhang J, et al. (2010) Nitro-oleic acid inhibits angiotensin II-induced hypertension. *Circ Res* 107(4):540–548.
28. Toledo E, et al. (2013) Effect of the Mediterranean diet on blood pressure in the PREDIMED trial: Results from a randomized controlled trial. *BMC Med* 11:207.
29. Burgoyne JR, Oviosu O, Eaton P (2013) The PEG-switch assay: A fast semi-quantitative method to determine protein reversible cysteine oxidation. *J Pharmacol Toxicol Methods* 68(3):297–301.
30. Schopfer FJ, et al. (2009) Detection and quantification of protein adduction by electrophilic fatty acids: Mitochondrial generation of fatty acid nitroalkene derivatives. *Free Radic Biol Med* 46(9):1250–1259.
31. Gomez GA, Morisseau C, Hammock BD, Christianson DW (2006) Human soluble epoxide hydrolase: structural basis of inhibition by 4-(3-cyclohexylureido)-carboxylic acids. *Protein Sci* 15(1):58–64.
32. Lim DG, et al. (2002) Nitrolinoleate, a nitric oxide-derived mediator of cell function: Synthesis, characterization, and vasomotor activity. *Proc Natl Acad Sci USA* 99(25):15941–15946.
33. Lima ES, et al. (2005) Nitrated lipids decompose to nitric oxide and lipid radicals and cause vasorelaxation. *Free Radic Biol Med* 39(4):532–539.
34. Oh JY, Giles N, Landar A, Darley-Usmar V (2008) Accumulation of 15-deoxy-delta (12,14)-prostaglandin J2 adduct formation with Keap1 over time: Effects on potency for intracellular antioxidant defence induction. *Biochem J* 411(2):297–306.
35. Kriska T, et al. (2013) Effect of human 15-lipoxygenase-1 metabolites on vascular function in mouse mesenteric arteries and hearts. *Prostaglandins Other Lipid Mediat* 106:8–15.
36. Siangjong L, Gauthier KM, Pfister SL, Smyth EM, Campbell WB (2013) Endothelial 12(S)-HETE vasorelaxation is mediated by thromboxane receptor inhibition in mouse mesenteric arteries. *Am J Physiol Heart Circ Physiol* 304(3):H382–H392.
37. Laursen JB, et al. (1997) Role of superoxide in angiotensin II-induced but not catecholamine-induced hypertension. *Circulation* 95(3):588–593.
38. Carluccio MA, et al. (2003) Olive oil and red wine antioxidant polyphenols inhibit endothelial activation: Antiatherogenic properties of Mediterranean diet phytochemicals. *Arterioscler Thromb Vasc Biol* 23(4):622–629.
39. Covas MI (2007) Olive oil and the cardiovascular system. *Pharmacol Res* 55(3):175–186.
40. Bonacci G, et al. (2012) Conjugated linoleic acid is a preferential substrate for fatty acid nitration. *J Biol Chem* 287(53):44071–44082.
41. Imig JD, Hammock BD (2009) Soluble epoxide hydrolase as a therapeutic target for cardiovascular diseases. *Nat Rev Drug Discov* 8(10):794–805.
42. Morisseau C, Hammock BD (2013) Impact of soluble epoxide hydrolase and epoxyeicosanoids on human health. *Annu Rev Pharmacol Toxicol* 53:37–58.
43. Barceló F, et al. (2009) Mediterranean-style diet effect on the structural properties of the erythrocyte cell membrane of hypertensive patients: The Prevencion con Dieta Mediterranea Study. *Hypertension* 54(5):1143–1150.
44. Lundberg JO, Carlström M, Larsen FJ, Weitzberg E (2011) Roles of dietary inorganic nitrate in cardiovascular health and disease. *Cardiovasc Res* 89(3):525–532.
45. Lundberg JO, Weitzberg E, Gladwin MT (2008) The nitrate-nitrite-nitric oxide pathway in physiology and therapeutics. *Nat Rev Drug Discov* 7(2):156–167.
46. Brestoff JR, Artis D (2013) Commensal bacteria at the interface of host metabolism and the immune system. *Nat Immunol* 14(7):676–684.
47. Lundberg JO, Weitzberg E (2013) Biology of nitrogen oxides in the gastrointestinal tract. *Gut* 62(4):616–629.
48. Huetteman DA, Bogie H (2009) Direct blood pressure monitoring in laboratory rodents via implantable radio telemetry. *Methods Mol Biol* 573:57–73.
49. Rudyk O, Prysyazhna O, Burgoyne JR, Eaton P (2012) Nitroglycerin fails to lower blood pressure in redox-dead Cys42Ser PKG1α knock-in mouse. *Circulation* 126(3):287–295.
50. Rudyk O, et al. (2013) Protein kinase G oxidation is a major cause of injury during sepsis. *Proc Natl Acad Sci USA* 110(24):9909–9913.
51. Yang J, Schmelzer K, Georgi K, Hammock BD (2009) Quantitative profiling method for oxylipin metabolome by liquid chromatography electrospray ionization tandem mass spectrometry. *Anal Chem* 81(19):8085–8093.

Supporting Information

Charles et al. 10.1073/pnas.1402965111

SI Methods

Generation of Cys521Ser Soluble Epoxide Hydrolase Knockin Mice. Mice constitutively expressing the soluble epoxide hydrolase (sEH) Cys521Ser mutation were generated on a pure C57BL/6 background by Taconic Artemis. A gene-targeting vector was constructed using C57BL/6-derived genomic DNA of the *Ephx2* gene from the RP23 BAC library. The Cys521Ser substitution was introduced into exon 18 using site-directed mutagenesis to change the TGT codon (National Center for Biotechnology Information (NCBI) reference sequence mouse: 13850) to TCC. A positive selection marker (Puromycin resistance, PuroR) was flanked by F3 sites and inserted into intro 16. Transfection of germ-line–competent C57BL/6N Tac ES cells with linearized and purified targeting vector DNA was then carried out. G418-mediated enrichment of ES cell clones that had integrated the targeting vector into their genome and Southern analysis of genomic DNA from G418-resistant ES cells with an *Ephx2* locus-specific probe yielded a number of candidate clones. Candidate clones were tested for correct homologous recombination at the target locus and the absence of additional integrations of the targeting vector by Southern analysis with targeting-vector–specific (internal) and target-locus–specific (external) probes in combination with multiple restriction digests. Injection of cells from one correctly targeted ES cell clone into wild-type (WT) blastocysts yielded male mice with 50–100% chimerism, as judged from coat color. Chimeric males with a high contribution of targeted ES cells were directly bred with a transgenic mouse line [C57BL/6-Tg(CAG-Flpe)2 Arte] ubiquitously expressing Flp recombinase under the control of the chicken β-actin promoter and a hCMV immediate early enhancer for germ-line transmission of the targeted *sEH* knockin allele and in vivo deletion of the flippase recognition target-flanked selection marker. The presence of the C43S point mutation was confirmed in both ES cells and mice heterozygous for the targeted *sEH* allele by sequencing of genomic DNA. Mice were maintained as stated in the Principles of Laboratory Animal Care published by the National Institutes of Health (NIH Publication Number 85–23). Experiments were approved by the King's College London Animal Welfare and Ethical Review Body. The sEH Cys521Ser mice were characterized by comparing them to their WT littermate controls as reported in Figs. 1–4 of this study. Additional characterization data are provided in Fig. S1 *A–C*.

Blood Biochemistry. Venous blood from WT or Cys521Ser KI mice were analyzed using a hand-held iSTAT analyzer, with EC8$^+$ cartridges (Abbott Laboratories).

Myography. Vascular rings were isolated from the mesenteric (second order) arteries. The rings were mounted in a tension myograph (Danish Myo Technology), stretched to the optimal pretension conditions (using a Danish Myo Technology Normalization Module), bathed in Krebs solution maintained at 37 °C and gassed with 95% CO_2:5% O_2 (vol/vol). During the vessel "wake up" phase, if vessels did not generate greater than 1 mN of force, they were rejected and the myograph channel was switched off. No vessels were rejected during subsequent analyses of the responses. Vasotone measurements of mesenteric vessels were made by determining the responses of U46619-contracted (0.1 μM; Sigma) vessels to nitro-oleic acid (NO$_2$-OA) (0– 10 μM). In some experiments, mesenteric vessels were incubated in 20 μM 1*H*-[1,2,4]oxadiazolo[4,3-*a*]quinoxalin-1-one (ODQ; Sigma) for 30 min before U46619 contraction and dose–response

to NO$_2$-OA. In some studies acetylcholine (dose–response; Sigma), L-N^G-nitroarginine methyl ester (L-NAME) (300 μM; Sigma) and indomethacin (10 μM; Sigma) was used. Tension experiments were carried out using at least three vessels per treatment intervention derived from at least three different WT or knockin (KI) mice.

Echocardiography. Age- and weight-matched littermate WT or Cys521Ser KI mice (four per group) were anesthetized and examined by echocardiography using a high-resolution Vevo 770 echocardiography system (VisualSonics) with a RMV-707B transducer running at 30 MHz. High-resolution, 2D brightness mode and motion-mode images at the level of the papillary muscles were obtained. Wall thickness and ventricular dimensions were measured and then left ventricular mass, ejection fraction, stroke volume, and cardiac output were calculated with Vevo Software (VisualSonics).

Telemetric Blood Pressure Monitoring in Vivo. Blood pressure (BP) was assessed by remote radiotelemetry in conscious freely moving mice. Briefly, mice were anesthetized with 2% isoflurane (Centaur Services) in 1 L of oxygen per minute with pre- and postoperative analgesia (buprenorphine, 0.1 mg per kg of body weight; Abbot Laboratories). A radiotelemetry probe catheter (TA11PA-C10, outside diameter of 0.4 mm; Data Science International) was implanted into the aortic arch of each mouse through the left carotid artery. After 1 wk of recovery, mice housed individually in cages were placed above the telemetric receivers with an output to a computer. Blood pressure was recorded by scheduled sampling for 10 s every 5 min (Dataquest LabPRO Acquisition system version 3.01; Data Sciences International). Baseline measurements were initiated after 1 wk postsurgery recovery and subsequent NO$_2$-OA, angiotensin (Ang) II, and saline delivery (below). A total of 7–12 WT or KI mice were studied per group to produce the average blood pressure data.

Ang II-Induced Hypertension and NO$_2$-OA Delivery. After baseline recordings (3 d) mice were again anesthetized and subjected to s.c. implantation of osmotic minipumps (model 1002; Alzet) for delivery of Ang II (Sigma) at an infusion rate of 1 mg/kg/day. After 3 d, a second osmotic minipump (model 1007D) containing either NO$_2$-OA at a concentration of 5 mg/kg/day or saline, was implanted s.c. A total of 7–12 WT or knockin mice were studied per group to produce the average blood pressure data. In some experiments, mice had only one osmotic minipump implanted with NO$_2$-OA or saline.

Soluble Epoxide Hydrolase Activity Assay. Mouse hearts from telemetered animals were rapidly isolated and frozen in liquid N$_2$ at the end of the BP monitoring protocol. Hearts were powdered under and stored in liquid nitrogen until ready for analysis. They were homogenized (1 mL of buffer per 100 mg of cardiac tissue) on ice in 100 mM Tri·HCl, pH 7.4 using a Polytron tissue grinder. Cytosolic fractions were prepared from the hearts by centrifugation at 25,000 × *g* for 5 min at 4 °C. A total of 20 μL of the cytosolic fraction was then used for the activity assay, adding it to 175 μL of 25 mM Tris·HCl, pH 7.4. After equilibration at room temperature, the reaction was initiated by the addition of 5 μL of 10 μM (3-phenyl-oxiranyl)-acetic acid cyano-(6-methoxy-naphthalen-2-yl)-methyl ester (PHOME; Cayman) dissolved in DMSO. The reaction mixture was left for 15 min, after which the fluorescence was monitored at 330/465 nm. In an additional reaction mixture, an sEH inhibitor [5 μL of 10-μM

12-(3-adamantan-1-yl-ureido)dodecanoic acid; Cayman] was added to ascertain the baseline reading for sEH activity for each sample.

Sample Preparation for Oxylipid Profiling Analysis. Plasma samples were spiked with 10 μL 500 nM internal standard I [d4-6-keto-prostaglandin F1a, d4-prostaglandin E2, d4-thromboxane2, d4-leukotriene B4, d11-14,15-dihydroxy-eicosatrienoic acid, d6-20-hydroxy-eicosatetraenoic acid (HETE), d4-9-hydroxy-octadecadie-noic acid, d8-12-HETE, d8-5-HETE, d11-11(12)-epoxy-eicosa-trienoic acid, d4-9(10)-epoxy-octadecenoic acid, d8-AA] and then were extracted by solid phase extraction using Oasis hy-drophilic-lipophilic-balanced (HLB) cartridges (3 cc 60 mg; Waters). The HLB cartridges were first washed with 2 mL ethyl acetate, 2 mL methanol twice, and 2 mL 95:5 vol/vol water/methanol with 0.1% acetic acid. The 6-mL plasma samples were then loaded onto the cartridges with 3-mL samples each time. The samples were then washed with 6 mL 95:5 vol/vol water/methanol with 0.1% acetic acid and dried for 20 min with low vacuum. The target analytes were then eluted with 0.5 mL meth-anol followed by 2 mL of ethyl acetate into the tubes with 6 μL 30% glycerol in methanol as the trap solution. The volatile sol-vents were evaporated by using vacuum centrifugation (SpeedVac) until 2 μL of trap solution remained in the tube. The residues were dissolved in 50 μL of methanol containing 200 nM in-ternal standard II (1-cyclohexyl-dodecanoic acid urea, CUDA). The samples were mixed with a vortex mixer for 2 min, centrifuged at $14,000 \times g$ for 5 min, and then transferred to autosampler vials with 150 μL inserts for liquid chromatography tandem MS (LC/MS/MS) analysis. LC/MS/MS analysis of oxylipids was per-formed using an Agilent 1200 SL liquid chromatography series (Agilent) with an Agilent Eclipse Plus C18 2.1×150 mm, 1.8-μm column for the oxylipins separation. The mobile phase A was water with 0.1% acetic acid, whereas the mobile phase B was composed of acetonitrile/methanol (80/15, vol/vol) and 0.1% acetic acid. Gradient elution was performed at a flow rate of 250 mL/min. The injection volume was 10 μL and the samples were kept at 4 °C in the autosampler. Analytes were detected by negative multiple reaction monitoring mode using a 4000 QTrap tandem mass spectrometer (Applied Biosystems) equipped with an electrospray ionization source (Turbo V). Calibration curves were generated by 10-μL injections of seven standards containing each analyte, internal standard I, and internal stan-dard II for quantification purposes.

Assay for Quantifying the Stoichiometry of NO₂-OA Adduction to sEH. This is based on a modified "PEG-switch" assay that allows the stoichiometry of reversible thiol oxidations to be determined using a Western blotting-based approach and an antibody to the protein of interest, namely sEH in these studies. The method, adapted to use β-mercaptoethanol (β-Me), as it allows reductive labeling of proteins that adduct NO₂-OA. Briefly, hearts from mice that had been subjected to 7 d of saline or NO₂-OA treatment from a minipump were rapidly isolated and frozen in nitrogen. Tissue samples were powdered under and stored in liquid nitrogen until subsequent analysis, when they were ho-mogenized (1 mL of buffer per 100 mg of cardiac tissue) on ice in 100 mM Tris·HCl, pH 7.4, 100 mM maleimide, and 1% SDS using a Polytron tissue grinder. The samples were heated at 50 °C for 25 min to alkylate-free cysteine thiols. The samples were desalted using spin columns (Pierce) and then 500 mM β-Me was added. The samples were heated at 37 °C for 60 min to reverse NO₂-OA adducts. The samples were desalted with a spin column again and 10 mM PEG-maleimide (Sigma) and 0.5% SDS were added to the sample, which was left rotating for 2 h at room temperature. A 2× SDS sample buffer [100 mM Tris·HCl, pH 6.8, 4% SDS (vol/vol), 20% glycerol (vol/vol), and 0.01% bro-mophenol blue] containing 100 mM maleimide was added to each sample. The samples were then resolved on a standard SDS/PAGE gel, Western blotted, and probed with an antibody for sEH (H-215, sEH antibody; Santa Cruz Biotechnology). GelPro Analyzer 3.1 was used to quantify the proportion of PEG-modified sEH to that of the reduced sEH.

Feeding Studies to Generate Endogenous Nitro Fatty Acids. Mice were gavaged daily for 5 d with conjugated linoleic acid (CLA, 10 mg/kg) and sodium nitrite (20 mg/kg) in 200 μL PEG 400. This protocol models concentrations of key components of the Mediterranean diet. Animals were killed 2 h after the last dose and tissues were rapidly isolated and frozen in liquid nitrogen. Control mice were gavaged with 200 μL PEG 400.

Fig. S1. Comparison of basal phenotype of WT and sEH KI mice. (*A*) Hematological analysis of WT and KI showed there were no differences in terms of WT and KI blood biochemical indices. (*B*) Myograph analysis showed there was no difference between either genotype in their vasodilatory responses to acetylcholine or acetylcholine in the presence of L-N^G-nitroarginine methyl ester (L-NAME) and indomethacin. (*C*) Echocardiographic analysis of cardiac function showed there were no differences in basal heart function parameters between WT and KI mice. LV mass, left ventricular mass; SV, stroke volume; EF, ejection fraction; FS, fractional shortening; CO, cardiac output; IVS, interventricular septum thickness; LVPW, left ventricular posterior wall thickness; LVAW, left ventricular anterior wall thickness; LVID, left ventricular internal dimension.